Assessment of Measures to Mitigate URN Emissions from Ships

Downloaded from: https://research.chalmers.se, 2026-11-07 10:50 UTC

Citation for the original published paper (version of record):
Everyd Bensow, R., Cianferra, M., Herrey, C. et al (2026). Assessment of Measures to Mitigate URN Emissions from Ships. Proceedings of the 9th Symposium on Marine Propulsors, smp'26

N.B. When citing this work, cite the original published paper.

research.chalmers.se offers the possibility of retrieving research publications produced at Chalmers University of Technology. It covers all kind of research output: articles, dissertations, conference papers, reports etc. since 2004. research.chalmers.se is administrated and maintained by Chalmers Library

(article starts on next page)

Ninth International Symposium on Marine Propulsors
smp'26, St. John's, Canada, July 2026

Assessment of Measures to Mitigate URN Emissions from Ships

Rickard Bensow[1], Marta Cianferra[2], Christopher Herrey[1], Qais Shehadeh Khraisat[1], Seo-Yoon Ryu[1]

[1]Chalmers University of Technology, Gothenburg, Sweden
[2]University of Trieste, Trieste, Italy

ABSTRACT

As underwater radiated noise emission from shipping has been acknowledged as an environmental pressure to the ocean, implementation of mitigation measures is in progress. To do this effectively, there is need to improve our methods to assess the effect of different measures, from the aspect of a regulating body as well as for ship owner and technical supplier. This paper will start by briefly reviewing studies on different measures and methods to assess the noise emissions. We will then focus on computational prediction methods and highlight some of the potential capabilities and issues in doing CFD-based assessment of ship noise. The radiated sound from cavitation on a sphere has been computed using both incompressible and compressible flow models, comparing different Ffowcs Williams and Hawkings (FW-H) set-ups, analysing the impact of neglecting flow compressibility and the choice of surfaces for sound source sampling. Attention is then shifted to the prediction of cavitation noise from a ship in full scale, again looking at different FW-H set-ups; instead of comparing with direct compressible predictions, sea-trial and model scale experimental data are available. For both studies, we note a high sensitivity to how the simulation is performed and the FW-H set-up towards predicted noise emissions. This sensitivity needs to be carefully considered when assessing different mitigation techniques.

Keywords

Underwater radiated noise, mitigation measures, propeller cavitation, Ffowcs Williams-Hawkings method, CFD, pressure pulses.

1 INTRODUCTION

Ambient underwater radiated noise from commercial shipping has increased over the past decades (McDonald et al., 2006; Frisk, 2012; Jalkanen et al., 2022) and is interfering with critical life functions of marine fauna (Erbe et al., 2019; Duarte et al., 2021). Continuous underwater noise emission from shipping is recognized as an environmental hazard and global initiatives push for mitigation of shipping noise (IMO, 2024). With the large variety in ship design and operation, mitigation measures need to be tailored to each case, forming a strong demand on accurate methods to assess the noise emission for vessels, during design, for the new built ship, during operation, and through maintenance over time. For most operation of merchant vessels, cavitation noise will typically dominate the noise spectrum (Cruz et al., 2021). Typical methods for this assessment include semi-empirical models, CFD predictions, model scale tests, and sea trials measurements. However, given the complex and demanding physics of the problem, neither accuracy or in general even precision in these methods are yet sufficient to make well-informed decisions on mitigation measures for general operation; relative ranking with the same method and team performing the analysis could however be expect to have a higher degree of reliability. Further, with the changing conditions the ship experiences during operation, e.g. with respect to adverse weather conditions, fouling, or varying bathymetry, there's a need to better understand and monitor underwater noise emissions continuously.

Dedicated sea trial measurements have been shown to give reasonably consistent results, but lack in control of the environmental properties governing the propagation from the ship to the measurement location. Further, they are naturally not suitable for early evaluation and choice of mitigation measures. Model scale tests are a common practice to obtain measurements of underwater radiated noise levels. However, such measurements are affected by uncertainties related to scaling, reverberations, and water quality (Tani et al., 2019, 2020). In addition, depending on the ratio between the cavitation tunnel size and ship model, blockage may influence both the flow and cavitation dynamics (Khraisat et al., 2026b).

Computational methods have been investigated for predicting underwater radiated noise, mainly through the use of semi-empirical or hybrid methods. Semi-empirical techniques are computationally cost-effective and suitable for early stage URN assessment (Lloyd et al., 2024a; Bosschers, 2018), though their predictive capability is often limited. Hybrid methods refer to the coupling of Computational Fluid Dynamics (CFD) with acoustic analogies, which have gained significant popularity in the maritime community. For bodies in motion such as a rotating propeller, the Ffowcs Williams and Hawkings (1969) (FW-H) acoustic analogy is most widely used. Due to the different

length and time scales in the acoustic problem compared with the flow problem, the coupling of CFD to an acoustic solver poses complications and direct computation of sound propagation in CFD, considering an accurate compressible flow description, is too costly. But as the FW-H analogy is originally developed for single-phase aeroacoustics, its application for multiphase cavitating flows has not been theoretically investigated and introduces additional challenges.

This paper will review some of the limitations of the FW-H approach and discuss different ways on how to increase the reliability of its CFD predictions on cavitation and the potential to use it to assess mitigation measures for underwater radiated noise emissions. First, a study of the canonical case of cavitation on a sphere will be presented, where high resolution simulations can be performed considering wave propagation, supporting the analysis of different FW-H approaches. Next, the study is extended to cavitating propeller operating in-behind condition, where we're limited to incompressible flow modelling and relaxed resolution in time and space. We will use this ship case to discuss the possibilities to assess the effect of different mitigation techniques.

2 REVIEW OF STUDIES ON URN MITIGATION MEASURES

Due to the negative impact of shipping noise on marine life, mitigation measures have been proposed in both literature and by global initiatives. The International Maritime Organization published a report in 2014 with recommended mitigation measures, pushing for quieter ship designs, optimal operational measures, standardized measurement procedures, and the evaluation of various implementation strategies (Cruz et al., 2021; IMO, 2024). Focusing on cavitation noise, from an intuitive understanding of the noise generating mechanisms, one can make the following notes:

- A speed reduction will yield reduced noise emissions as the power requirement reduces and the propeller gets unloaded. Exceptions may occur just above inception speed where cavitation may become more intermittent and dynamic, and if the propeller comes to operate at severe off-design conditions. An example of the latter is a CPP at pitch settings generating pressure side cavitation.
- Measures that allow for a more lightly loaded propeller will reduce noise emissions. This includes different energy saving technologies and maintenance efforts, such as hull cleaning.
- Creating a wake that is circumferentially homogeneous, minimizing cavitation dynamics, will reduce noise emissions.

However, in a typical propeller design task, there will naturally be a trade off between noise emissions and efficiency; the above comment on energy saving must be considered for the whole propulsion system.

de Jong et al. (2025) presented a framework for management of different environmental pressure with a focus on noise emissions, and found that vessel slow-down and hull and propeller cleaning are measures that have a potential to be effective and possible to implement on large scale. They found that technical mitigation measures are difficult to assess as they are dependent on the implementation on each individual vessel. The latter was discussed also by Andersson et al. (2023), where the Baltic strait was used for a case study and it was noted that during the year considered, more than 4000 vessels passed, thereby concluding that the general impact of implementing technical measures will be slow.

One of the earlier undertakings on noise mitigation was demonstrated by the port of Vancouver through the ECHO project. The project evaluated two different implementation strategies for ships approaching the harbor. One strategy by giving discount to vessels using certain underwater noise reducing technologies, and the other to asking vessels to reduce their speed (Vancouver Fraser Port Authority, 2018). Veirs et al. (2016) reported an approximate linear relation between speed and the source level. Similar reduced noise emissions with speed was noted by MacGillivray et al. (2019). While a reduction in speed increases the exposure time, the benefits of reducing the intensity outweigh the increased exposure time (Williams et al., 2019a; Andersson et al., 2023; Findlay et al., 2023). However, for certain vessels, like the coastal ferries studied by McIntyre et al. (2021), certain operating conditions at slow speed may lead to higher noise emissions. With respect to rerouting, Lalander et al. (2022) studied the effect of a change in shipping lane positions (due to traffic reasons) leading to a reduction in habitat quality for the marine wildlife. Other than these, practical studies on operational measures are rare, while a few hypothetical modeling studies have been performed (Williams et al., 2019b; Findlay et al., 2023).

Several technical solutions targeting propellers and cavitation have also been proposed and tested, but primarily at a low TRL level. Experimental studies have been performed to investigate the potential of propeller surface coatings as a mitigation measure (Korkut and Atlar, 2012; Bagheri et al., 2017). While results show noise reductions at certain frequencies due to delayed cavitation inception, the influence of scale effects is not considered as coating may have limited impact on cavitation at large scales. Other types of propeller blades surface texturing have been proposed with the aim of controlling tip vortex cavitation. Studies presented in (Asnaghi et al., 2021; Li et al., 2024) demonstrate the effectiveness of such techniques at reducing the vortex strength and delaying the onset of cavitation. A similar technical solution is the use of pressure-relief pores near the blade leading edge and tip to weaken vortex formation. While the experimental work by Aktas et al. (2020) indicates a reduction in noise levels at low-mid frequencies, additional mechanisms may increase broadband levels. The above techniques however come at a performance penalty that is non-negligible.

Blade design modification exploring winglets or optimized tip blade geometries have been investigated and presented in the literature. Moderate rake angles oriented towards the pressure side have been shown to effectively reduce tip vortex cavitation through numerical and experimental studies (Gao et al., 2019; Amini et al., 2019). Contracted and Tip Loaded (CLT) propellers have similarly been shown to be effective in reducing cavitation extent and pressure pulse levels compared with conventional designs (Gaggero et al., 2016). In practice however, many such designs suffer from dynamic and noise cavitation.

Wake improvement/modification devices have the potential to serve as a noise mitigation technology. The idea here is to obtain a more uniform distribution of the wakefield to and reduce the magnitude of the induced pressure fluctuations. A study on Pre-Swirl Stators, an energy saving device mainly intended to modify the wake vertical velocity component, is presented by Bensow (2015). The numerical results show that not only did the propeller performance improve, but the fluctuations of the propeller thrust are reduced. Similar potential has been reported for other energy saving devices, such as vortex generators (Saydam et al., 2018). In the SATURN project, a pump jet thruster was tested that showed improved noise performance (Grassi and Felli, 2024), where the gain can be expected to be a combination of the stator and the duct.

Injection-based systems have also been investigated as cavitation control or underwater radiated noise masking measures. The experimental study reported by Lee et al. (2018) showed that water injection through pores located at the blade tip suppresses tip vortex cavitation and reduces noise level by up to 20 dB. Similarly, Lloyd et al. (2024b) investigated air injection systems targeting both propeller and machinery noise through model scale experiments, and later application to full scale showed an overall noise reduction across the whole frequency range. Although many of these studies presented in the literature show promising results, quantitative studies on underwater radiated noise levels in real operation are scarce.

One useful component in mitigation of shipping noise could be through real-time onboard measurements of URN, which requires the estimation of the source-level using onboard sensors. Implementing an accurate tool for live-monitoring of URN would enable shipping crew to assess noise emissions continuously and adapt the operation of the ship when navigating in noise sensitive areas. Since cavitation typically dominates the noise spectrum at design speed, most research is focused on estimating the noise from cavitation, with various approaches. One approach is to use pressure sensors mounted on the hull above the propeller to estimate the source-level using beamforming (Jeong et al., 2021; Foeth and Bosschers, 2016). This approach is however sensitive to sensor placement and is less ideal for long term measurements due to build up of fouling on the pressure sensors. Another approach is to use hull mounted accelerometers and correlate onboard vibration levels to the cavitation source-level. Bosschers et al. (2023) estimated the source-level empirically through a transfer function based on the structural response of the aft hull. Other studies have proposed linear regression approaches, such as non-negative least squares and average quadratic velocity source level correlations (Larsen et al., 2021; Cintosun and Gilroy, 2021; Schottel, 2024).

There are many suggested mitigation measures that are still to be tested in practice. This includes hull cleaning techniques, energy saving measures, such as wind assisted propulsion, or technical measures. A missing aspect in literature is also the instantaneous operation of the vessel, where e.g. weather conditions and bathymetry affect the noise emissions; modelling aspect typically consider only ideal conditions in open water. Some of these are currently studied by the authors and will be presented in the future. A common aspect in all these is the need for accurate predictive tools to assess the effect of various techniques.

3 COMPUTATIONAL METHODS

3.1 Challenges in cavitation noise predictions

A prerequisite for predicting cavitation noise from shipping is to correctly model the cavitation extent and dynamics. Significant advances in simulation of cavitating flows have been made over the last two decades, ranging from interface resolving compressible simulations of bubble dynamics, through hybrid bubble-mixture models, to simplified models for engineering applications. For the usage considered here, one is limited to the latter, considering the scales of a ship in full scale. The mechanisms governing cavitation dynamics for cavitation erosion has been detailed by Bark and Bensow (2013), valid to a large extent also for noise emissions; some discussion related to sheet-tip vortex cavitation interaction was extended by Bosschers (2018). In short, four aspects need to be captured in the simulation: (1) the global cavity growth and collapse; (2) the development of re-entrant flow; (3) sheet-tip vortex cavitation interaction, and (4) tip vortex cavity dynamics. The first primarily affects first order blade passing frequency (BPF) harmonic and can be expected to be quite well predicted. The second and third influence largely the lower BPF harmonics, say up to the fifth BPF, but also some broadband content; provided wall normal resolution is good enough and the mesh around the initial part of the tip vortex is refined these mechanisms can be captured. Tip vortex cavity dynamics, in combination with an unsteady hull wake, is critical for the major broadband components in the signature; this has not yet been successfully predicted.

Early CFD predictions of cavitation on full-scale propellers are presented by Ji et al. (2010) using RANS modelling, managing predicting the first order pressure pulses. In model scale, Bensow and Bark (2010) showed well captured cavity dynamics, including reentrant flow and early tip vortex development using implicit LES. Using the same modelling technique, Lu et al. (2014) studied the requirements on wall resolution to capture the reentrant flow, however also only in model scale. Further studies in full scale were presented by, e.g., Li et al. (2018) and Sezen and Atlar (2023), using sufficient mesh resolution to capture mecha-

nisms (1)-(3) above. The tip vortex evolution is extremely challenging, modeling and mesh resolution issues are presented by Asnaghi et al. (2020); some dynamics of the tip vortex cavitation have however been captured and analysed in model scale by Ge et al. (2022) and in full scale by Khraisat et al. (2026b).

To compute the radiated noise generated by the predicted cavitation, further approximations and modeling is needed. Sound wave propagation is a compressible medium phenomena and follow different length scales compared with the cavitating flow. Thus a direct computation of the radiated noise within the flow solver is not feasible for ship applications. Also, extracting sound sources directly from the flow solver and propagate these directly in an acoustic solver is rare. Instead, propagation has been done through acoustic analogies via the Ffowcs Williams and Hawkings (FW-H) approach (Ffowcs Williams and Hawkings, 1969). As cavitation forms a volume source, an artificial integration surface commonly known as Permeable Data Surface (PDS) have been used without the need of computationally intensive volume integrals (Di Francescantonio, 1997). Using the hybrid acoustic approach for cavitation noise has two major unresolved issues. The first is that the FW-H method was developed for single phase flows and thus do not consider the dynamics of gas bubbles. It could be argued that using a PDS placed in pure liquid encompassing all sources one in practice applies the method to a single phase condition, but there are no theoretical exposition on this matter, nor detailed numerical studies; this argument relies on correctly capturing the pressure and velocity field inside the PDS. Secondly, using incompressible flow modeling leads to erroneous development of the pressure fields inside the PDS and the lack of a velocity perturbation in the FW-H terms, as shown numerically by Ahmed (2020) and Ge et al. (2022). Further studies by Vikström et al. (2022) showed that the prediction of cavitation noise by FW-H is heavily dependent on the PDS shape, with spherical surfaces indicating more consistent results. Previous studies on single-phase flow noise, e.g. Cianferra et al. (2019), indicate that the size and mesh resolution inside the PDS is critical for prediction quality. Care needs to be taken to avoid influence of numerical artifacts, from the cavitation modeling or mesh complications (e.g. Khraisat et al. (2026a)). All these issues are still not fully understood, nor always acknowledged. A possibly more robust approach was proposed by Wang et al. (2022), using the direct formulation of FW-H, considering the multiphase aspects of the problem, but this method has not been widely adopted.

3.2 Flow models

Cavitation flow simulations have here been performed with both compressible and incompressible solvers. The latter approach uses a transport equation based mixture approach with an explicit model for the mass transfer between liquid and gaseous water; here the Schnerr-Sauer model (Schnerr and Sauer, 2001) has been used. Depending on the case studied, both OpenFOAM and STAR-CCM+ have been used. Turbulence has been modeled with either RANS, using the $SST\ k-\omega$ model (Menter et al., 2003), or IDDES, using the Spalart-Almaras model (Shur et al., 2008). For the RANS simulations, the ad hoc Reboud correction (Reboud et al., 1998) was used in order to allow for dynamic cavitation behavior. This correction reduces the eddy viscosity in the mixture, effectively creating a hybrid RANS/LES method locally, allowing reasonably accurate cavitation predictions within an overall RANS framework. Further, the Boussinesq approximation is extended using a Quadratic Constitutive Relation (QCR) to account for turbulence anisotropy (Spalart, 2000) with non-linear terms for strain and vorticity rate tensors. The compressible simulations were conducted using the dbnsCavitatingFoam solver in OpenFOAM (Arabnejad and Bensow, 2020). This is a density-based solver that adopts the thermodynamic equilibrium mixture approach to model the presence of and phase transitions between liquid and vapor phases. Second-order convection schemes for velocity and turbulence are used.

3.3 Hydroacoustic modelling

The Ffowcs Williams and Hawkings (1969) acoustic analogy is an extension of Lighthill (1952) and Curle (1955) approaches, which accounts for sound sources from surfaces in motion. An inhomogeneous wave equation is derived by reformulation of the continuity and momentum equations, and uses the concept of generalized derivative and Heaviside function $H(f)$ to define the surfaces of the moving bodies.

$$\Box^2 p' = \frac{\partial}{\partial t}[\rho_o v_n \delta(f)] - \frac{\partial}{\partial x_i}[p n_i \delta(f)] + \frac{\partial^2}{\partial x_i \partial x_j}[H(f) T_{ij}] \tag{1}$$

where $\Box^2$ is the wave operator, ρ_o is the density of undisturbed medium, v_n is the velocity component normal to the surface, p is the gauge pressure on the surface, T_{ij} is the Lighthill stress tensor, n_i is a unit normal vector to the moving surface. The first term on the right-hand side of the equation represents the monopole (thickness) contributions and is dependent on the normal velocity component v_n to the surface. In the example of a non-cavitating rotating propeller, the thickness noise contribution is generated by pressure disturbances caused by the displaced fluid due to the blade rotation. The second term accounts for the dipole (loading) contributions, which are dominated by pressure disturbances p on the surface. The final term is the quadruple (volume) contributions which accounts for non-linear effects within the fluid volume. The quadruple term is computationally expensive, and in cases of low mach number flows, this term is typically dropped under the assumption that the contributions are small.

In the case of cavitating multiphase flows, the noise generated by cavitation is typically dominant, and one must account for these volume contributions. As discussed above, a virtual permeable data surface (PDS) is constructed in an attempt to avoid this complication. In this formulation, the FW-H equation can be written as,

$$\Box^2 p' = \frac{\partial}{\partial t}[\rho_o U_n]\delta(f) - \frac{\partial}{\partial x_i}[L_i \delta(f)] + \frac{\partial^2}{\partial x_i \partial x_j}[H(f) T_{ij}], \tag{2}$$

where,

$$U_n = \left(1 - \frac{\rho}{\rho_o}\right) v_n + \frac{\rho u_n}{\rho_o}, \tag{3}$$

$$L_i = p\delta_{ij} n_j + \rho u_i (u_n - v_n). \tag{4}$$

With this formulation, the monopole contributions now represents the mass flux across the permeable surface, while the dipole term represents the momentum flux across the surface and the local pressure forces acting on it. However, it is important to emphasizes that this formulation is problematic when combined an incompressible solver due to reasons discussed previously.

Given the limitations of the permeable FW-H formulation when applied to hydroacoustic applications, an alternative prediction methodology is considered in which cavitation volume dynamics are modelled as a monopole source. The solution of the wave equation in an unbounded domain for linear waves generated by a pulsating monopole source,

$$p(r,t) = \frac{\rho}{4\pi r} \ddot{V}(t - \frac{r}{c}), \tag{5}$$

where p is the acoustic pressure, r is the distance between the source and receiver, $\ddot{V}$ is the second order derivative of the cavitation volume. In the numerical simulation, time history data of the cavity volume evolution is collected at each time step. The data is then used to compute the second-order derivative central differencing scheme. However, as the cavity volume signal is discret, the numerical differentiation may introduce spurious fluctuations that contaminate the acoustic pressure signal. Therefore, to reduce these artificial fluctuations, the Locally Weighted Scatterplot Smoothing (LOWESS) method is applied to the vapor volume data before differentiation.

4 CASE STUDIES

4.1 Cavitating sphere

4.1.1 Motivation and objectives

The cavitating flow around a sphere is chosen as an idealized canonical benchmark case to investigate the relation between cavitation dynamics, collapse-induced pressure fluctuations, and the resulting acoustic response, as well as different approaches to compute the radiated sound. Owing to its simple geometry, the configuration allows the underlying physical mechanisms of cloud cavitation to be analyzed while minimizing geometric complexity, it's possible to consider an effectively open-domain configuration, which is advantageous for studying pressure-wave propagation with reduced confinement effects. Further, it's feasible to do high resolution compressible simulations that may provide a numerical reference avoiding measurement uncertainties related to near field measurement locations and reverberation characteristics of the test facility. Thus, the case will be used to perform systematic comparisons between compressible simulations that directly compute the acoustic wave propagation and acoustic predictions obtained from permeable FW-H formulations. Both incompressible and compressible flow solutions can be considered as inputs to the FW-H analysis in order to evaluate the influence of flow compressibility and PDS shape on the predicted acoustic response.

4.1.2 Case set-up

The numerical configuration reproduces the cavitating flow around a sphere in a water-tunnel environment under developed cloud-cavitation conditions, with a cavitation number of $\sigma = 0.4$. The sphere has a diameter of 0.15 m and the inflow velocity is 10 m/s, resulting in $Re = 1.5 \times 10^6$. The computational domain consists of a rectangular tunnel section with uniform inflow velocity and pressure-controlled outlet conditions defining the cavitation number. Slip-wall boundary conditions are applied at the lateral boundaries, while the sphere surface is treated as a non-slip wall. For compressible simulations, the computational domain is extended in the downstream and lateral directions to allow the propagation of collapse-induced pressure waves and to reduce artificial reflections.

Unstructured oct-tree type meshes were created with a body fitted prism layer extruded from the sphere surface. A mesh resolution study has been performed, varying both the refinement zones behind the sphere and the wall normal distribution in the prism layer. The results presented below are generated with a fine wake resolution and $y^+ \approx 30$, total cell count is around 44.5 million cells.

For acoustic analysis, several PDSs of different shapes and spatial extents are defined around the cavitation region as shown in Figure 1. Pressure signals are recorded at selected near- and far-field receiver locations and subsequently analyzed in the frequency domain; in this paper results from a receiver point 10 m downstream of the sphere are shown.

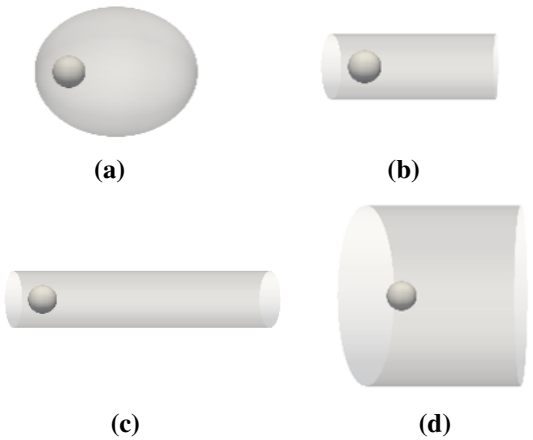

Figure 1: The four PDSs that are used in the acoustic analysis: (a) Ellipsoid, (b) short cylinder, (c) long cylinder, and (d) wide cylinder.

4.1.3 Results and discussion

To validate the numerical framework, the predicted cavitation dynamics are compared with available experimental visualizations of cloud cavitation around the sphere. The numerical results reproduce the main stages of the cavitation cycle, including cavity growth, cloud shedding, and downstream collapse. The overall cavity extent and temporal evolution show good qualitative agreement with the experimental observations.

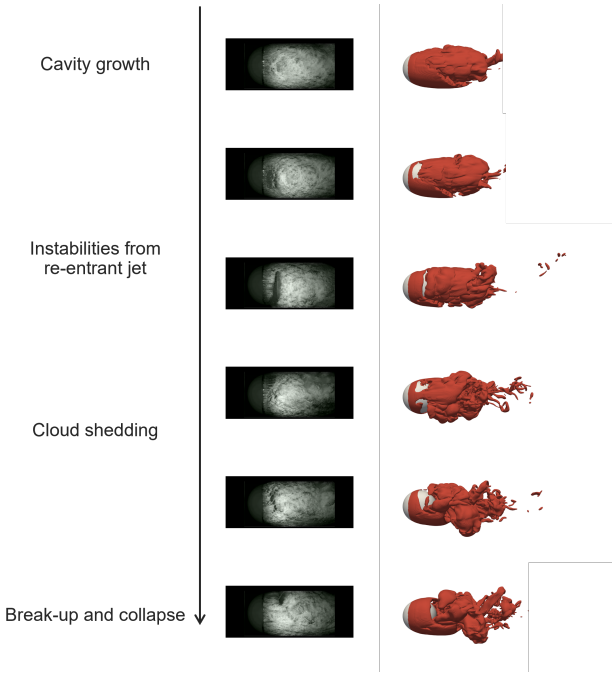

Figure 2: Comparison of experimental high-speed visualizations (left, reproduced from Brandner et al. (2010)) and numerical predictions (right) fo3 vapor volume fraction isosurfaces over one cavitation cycle at $\sigma = 0.4$.

Here, we briefly present just the predicted power spectral density (PSD) at the chosen receiver point. Figure 3 includes results derived from all four PDSs based on both compressible and incompressible solutions, as well as from the vapour volume acceleration. We remark that the compressible simulation, at this stage, is not run long enough to have fully converged statistics so the results should be interpreted with care.

For the simulated condition, the cavitation is very dynamic and a regular shedding of the main cavity is not clearly seen. The acoustic signal is thus of a rather even broadband character. Still, it's clear that the results depend highly on simulation approach and choice of PDS. The main conclusion is that there is a spread in predicted PSD from the incompressible simulation between the different PDSs; in some frequency ranges this amounts to several orders of magnitude. This is not the case for the compressible simulation, where all permeable data sampling surfaces yields very similar results. These results indicate that it will be difficult to judge an analysis of mitigation measures from incompressible FWH-results unless the set-ups are identicals, while comparisons to measurements or regulations will be questionable. Also, the analysis based on the volume acceleration show results that overall are of the right order of magnitude; there is one sharp dip at 800 Hz which is believed to be related to the LOWESS treatment of the cavity volume signal although a similar drop is present in the compressible simulation result as well.

Noteworthy is also that the compressible simulation leads to much smoother spectra, while the incompressible simulations show much more jagged curves. This is independent of the PDS. The reason for this is unknown. We have previously noted that the pressure field may show seemingly spurious peaks when simulating cavitating flows using an incompressible flow model. This has not been a noted problem in this simulations, but potentially it exists at a lower intensity and show up only in the acoustic signal.

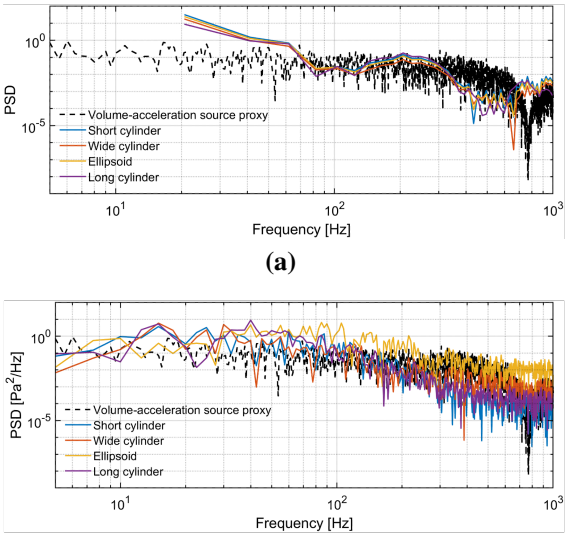

Figure 3: Comparison of FW-H predicted acoustic spectra for different PDS surfaces. Panel (a) shows results based on compressible simulations and panel (b) shows incompressible simulations; black lines computed from the cavity volume acceleration term.

4.2 Coastal tanker

4.2.1 Motivation and objectives

A fully appended ship of a modern cargo vessel is numerically investigated. The vessel is equipped with a single controllable-pitch, four-bladed propeller with moderate skew. Measurements on underwater radiated noise are available from sea trial measurements performed by the Swedish Environmental Research Institute (IVL) and Kongsberg Maritime. Model scale tests have also been carried out at the Research Institutes of Sweden (RISE). The vessel will be used for extensive studies related to noise emissions in several ongoing projects, including effects of slow down, wind assisted propulsion, propeller pitch control, and on-board noise monitoring; this concerns both measurements and computations. In this paper we will focus on the baseline configuration and the predictive accuracy of the ship signature, while new results for the dif-

ferent mitigation techniques will be published as they become available. The full description of the analysis of the baseline case is presented by Bensow et al. (2025) and the detailed computations in Khraisat et al. (2026a).

4.2.2 Case set-up

The ship geometry is placed in a computational domain with dimensions defined based on the ship length between perpendiculars (Lpp). Standard boundary conditions are applied with a velocity inlet, a pressure outlet, and slip walls on the remaining domain boundaries. Simulations are performed using the commercial software package Simcenter STAR-CCM+/2410 (double-precision). Propeller rotation is modelled using the sliding mesh approach, where the computational domain is divided into subdomains connected with an interface, and are discretized with the built-in meshing tools. A mean y^+ distribution below 1 is maintained on the propeller blades and hub to resolve the boundary layer. For the hull and rudder surfaces, the wall function approach is used for numerical stability reasons. The all-y^+ formulation is applied, which uses blending functions for turbulent kinetic energy production and dissipation. In the transient computations, the time step size corresponds to $0.25°$ of a propeller revolution with 15 inner iterations per time step.

Three different PDSs are considered for comparison. Based on the conclusions of Vikström et al. (2022), only spherical surfaces are used with radii $1.4R$, $2R$, and $5R$ respectively, where R is the propeller radius; the smallest is defined centered around the shaft line location and the the two larger at the blade tip at top position, the approximate sound source location. In total 410 receiver points have been analysed at various distances and positions, circumferentially, radially, and longitudinally.

4.2.3 Results and discussion

First, the influence of the choice of PDS on the predicted radiated noise level (RNL) is presented. Figure 4 presents results for all three surfaces, both as closed and with the section of the sphere where the propeller slip passes the surface, denoted as end-cap, removed. Two observations can be made: The first is that the primary effect of the end-cap is a general shift in the RNL, with only minor frequency dependence. The second is that, in some frequency ranges, there are significant differences between the prediction based on the different surfaces. The dramatic difference is in the high frequency range, where the two smaller surfaces give an un-physical increase in RNL above around 300 Hz. The behavior is similar to what was noted by Ge et al. (2022) and Vikström et al. (2022), but was here due to different reasons, at least partly; high frequency numerical disturbances were noted in the FW-H source terms that could be deduced to come from the sliding interface around the rotating propeller. The discrepancy just below 100 Hz, however, is related to the radiation from the imprinted pressure field on the hull above the propeller, which forms an important contribution as will be further commented below; the smaller PDSs do not fully enclose this noise source and thus not captured in the FW-H based on these surfaces. For the rest of the discussion, thus only the $5R$ PDS will be considered.

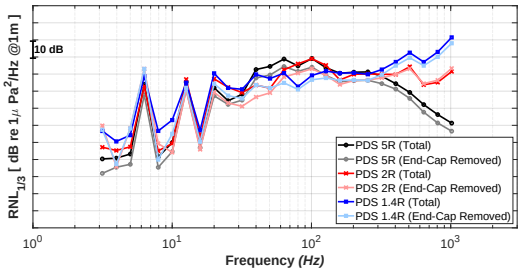

Figure 4: Radiated noise levels from all permeable data surfaces with and without end-cap.

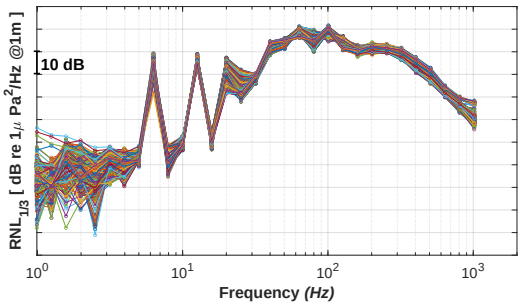

Figure 5: Sound pressure spectral density level from the 5R PDS for all receivers. Distance normalization is applied assuming spherical spreading losses.

We now remark that the predicted RNL show a dependence on the receiver location. Combining the predictions from all receivers yields Figure 5. The physical directivity is unfortunately not known. Cavitation develops on the propeller only close to the top position in the hull wake, but the collapse dynamics, forming the main noise source, occurs somewhat to the port side of the vessel. The predictions show a spread of up to 20 dB between different receivers in the range between the 3rd and 5th BPF, and then around 5 dB across the range of higher frequencies. If this large spread would be physical, it shows both that the simple homogeneous source models often used for sound maps can be severly erroneous and that care most be taken in choosing receiver location, in measurements as well as in numerical predictions. We believe however it is mainly due to numerical artefacts with the FW-H approach.

To better understand the source contribution, the different terms in the FW-H integrals can be analysed. For the permeable FW-H analysis, the thickness and loading terms are computed from the $5R$ PDS. As shown in the top plot in Figure 6, the thickness term is dominant for the harmonic contribution at the first threee BPF, while the loading term dominates in the broadband range. To explain this, also the contributions from the solid FW-H, i.e. when evaluated on the different ship surfaces, are shown in the bottom plot. For this cavitating condition, we note that the RNL from the propeller surface is not correct, due to that parts of the blades are cavitating. The rudder gives a very minor contri-

bution, but the hull show a significant level above 300 Hz; a further split of the hull surface show that it's only the aft surface that contributes. Thus, the aft hull surface radiates sound as a dipole, given that this source shows up as a loading term, and stems from the transient pressure field on the hull due to the propeller rotation.

Finally, in Figure 7 we present the source level (SL) as predicted in sea trials, model tests (RISE) and simulations, using both the permeable FW-H and the cavity volume acceleration analogy; the latter is combined with the solid FW-H prediction on the aft hull surface and denoted A-N + S-FWH in the following. Also results from model scale (MS) simulations in two domains are shown in the figure. Overall, the accuracy is disappointing. During the sea trials, engine vibrations were registered and it can be concluded that large discrepancy below 50 Hz is due to engine noise contribution. There are up to 20 dB differences for several frequency ranges, where only in some cases an explanation can be given.

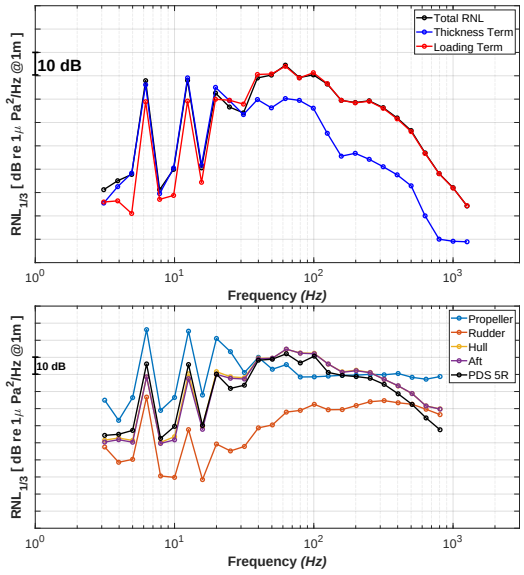

Figure 6: Thickness and Loading terms as computed from the permeable data surface 5R (top). RNL predictions using different solid impermeable data surfaces under cavitating condition (bottom).

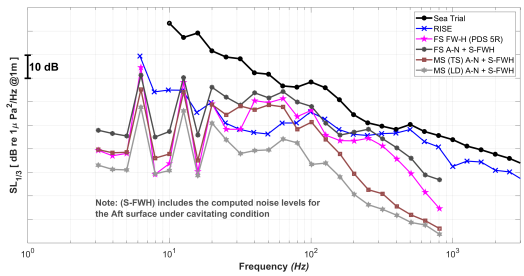

Figure 7: Source Noise Level from experimental measurement and the hybrid A-N method for model and full scale conditions.)

5 CONCLUSIONS

The objectives of this work have been to understand the complications of predicting cavitation noise, and improve the accuracy and precision of engineering CFD assessment of mitigation measures for ship generated noise emissions. This has unfortunately not been met, yet, and the studies are still in progress. The cavitating sphere case is believed to be a suitable canonical case for continued analysis of computational hydroacoustics, and the results will be further expanded beyond the scope of this paper, including comparisons between direct acoustic predictions, using the compressible flow model, with FWH-predictions.

Considering the tanker case, we believe that no absolute prediction of the effect of mitigation techniques can be done with any method today, possibly with the exception of deep water sea trials. We have high hopes that carefully performed CFD simulations will have the precision to at least rank different measures, be it of technical or operational types. Given the reported sensitivity to how the simulation is performed and to the shape and size of the PDS, comparing results from different organisations or studies are deemed problematic. More studies are needed to be able to formulate best practice guidelines that reduces this sensitivity and increase the reliability in numerical predictions of radiated underwater noise emissions.

ACKNOWLEDGEMENTS

Funding for this work has been provided by the Lighthouse program in Sustainable Shipping (projects PUB and PUB-TVÅ), the Swedish Transportation Agency (project BOUB), the EU Sustainable Blue Economy Partnership (project BluEcho), and Kongsberg Maritime AB (through the UTC in Computational Hydrodynamics at Chalmers).

The computations were enabled by resources provided by Chalmers e-Commons at Chalmers and by the National Academic Infrastructure for Supercomputing in Sweden (NAISS) at NSC partially funded by the Swedish Research Council through grant agreement no. 2022-06725.

REFERENCES

Ahmed, S. (2020), "On the noise generated by a ship propeller," PH.D. dissertation, UNSW Sydney.

Aktas, B., Yilmaz, N., Atlar, M., Sasaki, N., Fitzsimmons, P., and Taylor, D. (2020), "Suppression of Tip Vortex Cavitation Noise of Propellers using PressurePoresTM Technology," Journal of Marine Science and Engineering, 8(3).

Amini, A., Reclari, M., Sano, T., et al. (2019), "Suppressing tip vortex cavitation by winglets," Experimental Fluids, 60, 159.

Andersson, M., Bensow, R., Glebe, D., Hassellöv, I.-M., Lalander, E., Langlet, D., Larsson, K., Malmberg, L., Sundblad, E.-L., and Svedendahl, M. (2023), "Management Measures to Reduce Continuous Underwater Noise from Shipping,"

Arabnejad, M. H. and Bensow, R. E. (2020), "dbnsCavitatingFoam: A density-based solver with equilibrium cavitation models in the OpenFOAM framework," .

Asnaghi, A., Svennberg, U., and Bensow, R. E. (2020), "Large Eddy Simulations of cavitating tip vortex flows," Ocean Engineering, 195, 106703.

Asnaghi, A., Svennberg, U., Gustafsson, R., and Bensow, R. E. (2021), "Propeller tip vortex mitigation by roughness application," Applied Ocean Research, 106, 102449.

Bagheri, M. R., Ms, S., and Mehdigholi, H. (2017), "An Experimental Study on the Effect of IS700 Coating on the CavitationInception and Development, and Noise Reduction of a Marine Propeller," Journal of Applied Mechanical Engineering, 6, 1-7.

Bark, G. and Bensow, R. (2013), "Hydrodynamic mechanisms controlling cavitation erosion," International Shipbuilding Progress, 60(1-4).

Bensow, R. and Bark, G. (2010), "Implicit LES predictions of the cavitating flow on a propeller," Journal of Fluids Engineering, Transactions of the ASME, 132(4).

Bensow, R., Khraisat, Q. S. A., Johansson, T., Andersson, C., Andersson, M., Linné, M., Hallander, J., Liefvendahl, M., Kämpeskog, A., Persson, M., and Sigray, P. (2025), "PUB – Methods to predict radiated ship noisee," , Lighthouse report.

Bensow, R. E. (2015), "Large eddy simulation of a cavitating propeller operating in behind conditions with and without pre-swirl stators," Proceedings of the 4th International Symposium on Marine Propulsors, Austin, TX, USA, volume 4.

Bosschers, J. (2018), "A semi-empirical prediction method for broadband hull-pressure fluctuations and underwater radiated noise by propeller tip-vortex cavitation," Journal of Marine Science and Engineering, 6(49).

Bosschers, J., Koning, J., and Schouten, R. (2023), "Estimation of the Underwater Radiated Noise by Ship Propeller Cavitation Using Onboard Sensors," Proceedings of the 29th International Congress on Sound and Vibration (ICSV29), International Institute of Acoustics and Vibration (IIAV), 1–8.

Brandner, P. A., Walker, G. J., Niekap, P. N., and Anderson, B. (2010), "An experimental investigation of cloud cavitation about a sphere," Journal of Fluid Mechanics, 656, 147–176.

Cianferra, M., Ianniello, S., and Armenio, V. (2019), "Assessment of methodologies for the solution of the Ffowcs Williams and Hawkings equation using LES of incompressible single-phase flow around a finite-size square cylinder," Journal of Sound and Vibration, 453, 1–24.

Cintosun, E. and Gilroy, L. (2021), "Estimating Ship Underwater Radiated Noise from Onboard Vibrations," D031S011R003.

Cruz, E., Lloyd, T., Bosschers, J., Lafeber, F. H., Vinagre, P., and Vaz, G. (2021), "Study on Inventory of Existing Policy, Research and Impacts of Continuous Underwater Noise in Europe," Prepared by WavEC Offshore Renewables and Maritime Research Institute Netherlands.

Curle, N. (1955), "The influence of solid boundaries upon aerodynamic sound," Proceedings of the Royal Society of London. A. Mathematical and Physical Sciences, 231(1187), 505-514.

de Jong, K., Murray, C. C., Anabitarte, A., Bailey, S., Drake, L., Fernandes-Salvador, J. A., Hassellov, I. M., Heibeck, N., Jalkanen, J. P., Lehikoinen, A., Merchant, N., Nylund, A. T., and Redfern, J. V. (2025), "Trade-offs and synergies in the management of environmental pressures: a case study on ship noise mitigation," Marine Pollution Bulletin, 218(April), 118073.

Di Francescantonio, P. (1997), "A NEW BOUNDARY INTEGRAL FORMULATION FOR THE PREDICTION OF SOUND RADIATION," Journal of Sound and Vibration, 202(4), 491-509.

Duarte, C. M., Chapuis, L., Collin, S. P., Costa, D. P., Devassy, R. P., Eguiluz, V. M., Erbe, C., Gordon, T. A. C., Halpern, B. S., Harding, H. R., Havlik, M. N., Meekan, M., Merchant, N. D., Miksis-Olds, J. L., Parsons, M., Predragovic, M., Radford, A. N., Radford, C. A., Simpson, S. D., Slabbekoorn, H., Staaterman, E., Opzeeland, I. C. V., Winderen, J., Zhang, X., and Juanes, F. (2021), "The soundscape of the Anthropocene ocean," Science, 371(6529), eaba4658.

Erbe, C., Marley, S. A., Schoeman, R. P., Smith, J. N., Trigg, L. E., and Embling, C. B. (2019), "The Effects of Ship Noise on Marine Mammals—A Review," Frontiers in Marine Science, 6.

Ffowcs Williams, J. E. and Hawkings, D. L. (1969), "Sound generation by turbulence and surfaces in arbitrary motion," Philosophical Transactions of the Royal Society of London. Series A, Mathematical and Physical Sciences, 264(1151), 321–342.

Findlay, C. R., Rojano-doñate, L., Tougaard, J., Johnson, M. P., and Madsen, P. T. (2023), "Small reductions in cargo vessel speed substantially reduce noise impacts to marine mammals," Science Advances, 2987(June).

Foeth, E. J. and Bosschers, J. (2016), "Localization and Source-Strength Estimation of Propeller Cavitation Noise Using Hull-Mounted Pressure Transducers," Proceedings of the 31st Symposium on Naval Hydrodynamics, Office of Naval Research.

Frisk, G. V. (2012), "Noiseonomics: The relationship between ambient noise levels in the sea and global economic trends," Scientific reports, 2(1), 437.

Gaggero, S., Gonzalez-Adalid, J., and Sobrino, M. P. (2016), "Design and analysis of a new generation of CLT propellers," Applied Ocean Research, 59, 424-450.

Gao, H., Zhu, W., Liu, Y., and Yan, Y. (2019), "Effect of various winglets on the performance of marine pro-

peller," Applied Ocean Research, 86, 246-256.

Ge, M., Svennberg, U., and Bensow, R. E. (2022), "Investigations on prediction of ship noise using the FWH acoustic analogy with incompressible flow input," Ocean Engineering, 257, 111531.

Grassi, A. D. and Felli, M. (2024), "SATURN Deliverable 4 . 2 on source level and propulsive efficiency . source level and propulsive efficiency," , SATURN project, Deliverable 4.2.

IMO (2024), "Revised Guidelines for the Reduction of Underwater Radiated Noise from Shipping to Address Adverse Impacts on Marine Life," , International Maritime Organization, effective 1 December 2024. This circular revokes MEPC.1/Circ.906.

Jalkanen, J.-P., Johansson, L., Andersson, M. H., Majamäki, E., and Sigray, P. (2022), "Underwater noise emissions from ships during 2014–2020," Environmental Pollution, 311, 119766.

Jeong, H., Lee, J.-H., Kim, Y.-H., and Seol, H. (2021), "Estimation of the Noise Source Level of a Commercial Ship Using On-Board Pressure Sensors," Applied Sciences, 11(3).

Ji, B., wu Luo, X., lin Wu, Y., hong Liu, S., yuan Xu, H., and Oshima, A. (2010), "Numerical investigation of unsteady cavitating turbulent flow around a full scale marine propeller," Journal of Hydrodynamics, Ser. B, 22(5, Supplement 1), 747-752.

Khraisat, Q. S. A., Persson, M., and Bensow, R. E. (2026a), "Cavitation underwater radiated noise methodology applied to a propeller operating in-behind condition Citation for the original published paper (version of record): operating in-behind condition," Ocean Engineering, 349, 124084.

Khraisat, Q. S. A., Persson, M., and Bensow, R. E. (2026b), "Scale effects on marine cavitating flows : A study on a hydrofoil and a propeller operating in-behind condition Citation for the original published paper (version of record): propeller operating in-behind condition," Ocean Engineering, 351(P1), 124310.

Korkut, E. and Atlar, M. (2012), "An experimental investigation of the effect of foul release coating application on performance, noise and cavitation characteristics of marine propellers," Ocean Engineering, 41, 1-12.

Lalander, E., Nordström, R. L., and Andersson, M. (2022), "Changes in the underwater soundscape in Kattegat due to shipping re-routing," November, FOI report FOI-R–5334–SE.

Larsen, G., Dupuis, J., and Gilroy, L. (2021), "Results from Off-Board Noise Prediction Study in ORCA-Class Training Vessel," .

Lee, C. S., Ahn, B. K., Han, J. M., et al. (2018), "Propeller tip vortex cavitation control and induced noise suppression by water injection," Journal of Marine Science and Technology, 23, 453–463.

Li, D. Q., Hallander, J., and Johansson, T. (2018), "Predicting underwater radiated noise of a full scale ship with model testing and numerical methods," Ocean Engineering, 161(June 2017), 121–135.

Li, Y., Zhang, L., Deng, F., Qin, X., and Zhao, D. (2024), "Tip vortex suppression by using dimpled roughness," Ocean Engineering, 299, 117348.

Lighthill, M. J. (1952), "On sound generated aerodynamically I. General theory," Proceedings of the Royal Society of London. A. Mathematical and Physical Sciences, 211(1107), 564-587.

Lloyd, T., Daniel, J., Bosschers, J., and Schuster, M. (2024a), "' PIANO ': A physics-based semi-empirical source level model for fleet-scale ship URN prediction," 8th Symposium on Marine Propulsors, March, Berlin, Germany.

Lloyd, T., Lafeber, F. H., and Bosschers, J. (2024b), "Ship URN mitigation by air injection: model-scale experiments and application to full-scale measurement data," Proceedings of the Eighth International Symposium on Marine Propulsors (smp'24).

Lu, N. X., Bensow, R. E., and Bark, G. (2014), "Large eddy simulation of cavitation development on highly skewed propellers," Journal of Marine Science and Technology (Japan), 19(2).

MacGillivray, A. O., Li, Z., Hannay, D. E., Trounce, K. B., and Robinson, O. M. (2019), "Slowing deep-sea commercial vessels reduces underwater radiated noise," The Journal of the Acoustical Society of America, 146(1), 340–351.

McDonald, M. A., Hildebrand, J. A., and Wiggins, S. M. (2006), "Increases in Deep Ocean Ambient Noise in the Northeast Pacific West of San Nicolas Island, California," The Journal of the Acoustical Society of America, 120(2), 711–718.

McIntyre, D., Lee, W., Frouin-Mouy, H., Hannay, D., and Oshkai, P. (2021), "Influence of propellers and operating conditions on underwater radiated noise from coastal ferry vessels," Ocean Engineering, 232(September 2020).

Menter, F. R., Kuntz, M., Langtry, R., et al. (2003), "Ten years of industrial experience with the SST turbulence model," Turbulence, heat and mass transfer, 4(1), 625–632.

Reboud, J.-L., Stutz, B., and Coutier, O. (1998), "Two phase flow structure of cavitation: experiment and modeling of unsteady effects," 3rd international symposium on cavitation CAV1998, Grenoble, France, volume 26, 1–8.

Saydam, A. Z., Gokcay, S., and Insel, M. (2018), "CFD based vortex generator design and full-scale testing for wake non-uniformity reduction," Ocean Engineering, 153, 282-296.

Schnerr, G. H. and Sauer, J. (2001), "Physical and numerical modeling of unsteady cavitation dynamics," Fourth international conference on multiphase flow, volume 1,

ICMF New Orleans New Orleans, LO, USA.

Schottel (2024), "Hydrodynamic Propeller Noise Monitoring System -HyPNoS," .

Sezen, S. and Atlar, M. (2023), "Marine propeller underwater radiated noise prediction with the FWH acoustic analogy Part 2: Assessment of model scale propeller hydroacoustic performance under non-uniform flow conditions," Ocean Engineering, 270(September 2022), 113443.

Shur, M. L., Spalart, P. R., Kh, M., and Travin, A. K. (2008), "International Journal of Heat and Fluid Flow A hybrid RANS-LES approach with delayed-DES and wall-modelled LES capabilities," International Journal of Heat and Fluid Flow, 29(6), 406–417.

Spalart, P. (2000), "Strategies for turbulence modelling and simulations," International Journal of Heat and Fluid Flow, 21(3), 252-263.

Tani, G., Viviani, M., Felli, M., Lafeber, F. H., Lloyd, T., Aktas, B., Atlar, M., Turkmen, S., Seol, H., Hallander, J., and Sakamoto, N. (2020), "Noise measurements of a cavitating propeller in different facilities: Results of the round robin test programme," Ocean Engineering, 213(March), 107599.

Tani, G., Viviani, M., Ferrando, M., and Armelloni, E. (2019), "Aspects of the measurement of the acoustic transfer function in a cavitation tunnel," Applied Ocean Research, 87, 264-278.

Vancouver Fraser Port Authority (2018), "ECHO Program Voluntary Vessel Slowdown Trial – Summary Findings," , Vancouver Fraser Port Authority, Vancouver, BC.

Veirs, S., Veirs, V., and Wood, J. D. (2016), "Ship noise extends to frequencies used for echolocation by endangered killer whales," PeerJ, 4, e1657.

Vikström, M., Svennberg, U., Ge, M., and Bensow, R. E. (2022), "The Effect of Porous Data Surface Shape and Size on Ship Noise Prediction using the FWH Acoustic Analogy with Incompressible Solver for a Cavitating Propellers," Proceedings of the 7th International Symposium of Marine Propulsors.

Wang, Y., Mikkola, T., and Hirdaris, S. (2022), "A fast and storage-saving method for direct volumetric integration of FWH acoustic analogy," Ocean Engineering, 261(June), 112087.

Williams, R., Veirs, S., Veirs, V., Ashe, E., and Mastick, N. (2019a), "Approaches to reduce noise from ships operating in important killer whale habitats," Marine Pollution Bulletin, 139, 459-469.

Williams, R., Veirs, S., Veirs, V., Ashe, E., and Mastick, N. (2019b), "Approaches to reduce noise from ships operating in important killer whale habitats," Marine Pollution Bulletin, 139(May 2018), 459–469.